CHEMISTRY OF MATERIALS

Article

pubs.acs.org/cm

Progress Report on the Generation of Polyfunctional Microscale Particles for Programmed Self-Assembly

Ryan Deschner,[†] Hao Tang,[†] Peter Allen,[‡,§] Cecilia Hall,[§] Rocco Hlis,[§] Andrew Ellington,[‡,§] and C. Grant Willson*[,†,§]

[†]Chemical Engineering Department, [‡]Institute for Cellular and Molecular Biology, and [§]Chemistry and Biochemistry Department, The University of Texas at Austin, Austin, Texas 78712, United States

Supporting Information

ABSTRACT: A process for 3D programmed self-assembly of lithographically printable microscale polymer particles using ssDNA hybridization as the associative force is described. We report our progress in establishing the unit processes required for 3D programmed self-assembly and demonstrate the successful fabrication and sequence-specific self-assembly of covalent ssDNA-functionalized parallelepipeds with dimensions in the sub 10 μm regime characterized by optical microscopy and imaging flow cytometry. This technology has the potential to produce parallelepiped particles with different ssDNA on each facet.

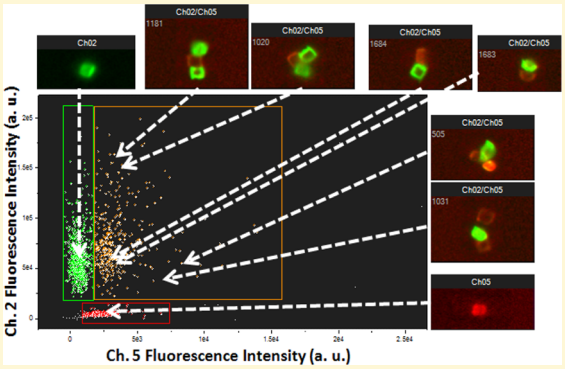

DNA-assisted self-assembly is an attractive technology that seeks to employ the highly specific and programmable nature of DNA hybridization as an associative force for generating highly ordered and complex arrangements of nanoscale and microscale materials. As the production of relatively error-free single-strand DNA (ssDNA) has become cheaper and more available up to lengths on the order of 50 bp, it has found rapidly increasing use in applications such as surface modification,[1,2] drug delivery,[3] biosensors,[4−6] and microelectronics.[7−9]

The power of DNA hybridization as a tool for the design of self-assembled structures derives from the binding specificity of the material. Directed or programmed self-assembly of ssDNA can produce junctions[10] and polyhedral cagelike structures[11] as well as highly complex shapes such as smiley faces and ornate map projections[12] in impressive yield. DNA can also be covalently linked to the surface of metallic and polymer nanoparticles to drive the formation of larger hybrid macrostructures such as chains,[13,14] 2D arrays,[15] and clusters.[16,17] ssDNA has also been attached to particles of different shapes that can be manipulated using centrifugation,[18] magnetic separation,[19−21] and dielectrophoresis[22] and easily measured using flow cytometry,[23] fluorescence microscopy,[24] surface plasmon resonance (SPR),[6] and UV−vis spectroscopy.[25] In addition, the formation of particles capable of localizing two different ssDNA sequences on their surfaces, so-called Janus particles,[26] has been shown to add increasing degrees of freedom to the design of self-assembling particle-DNA systems. Very recently, hydrogel cubes[27] were assembled using DNA, some facets of which were functionalized with different cross-linked "giant DNA" chains. Self-assembled T-junctions and 2D arrays were demonstrated with these materials. Similarly, basic monofunctionalized sets of silicon particles[7] were assembled using photolithography in conjunction with chemical etching. These advancements open the door to future technologies, which involve yet more complex particle shapes with many highly localized ssDNA functionalizations. However, as of the date of publication of this article, the authors know of no reports of a methodology for generating polyfaceted solid polymer particles that are capable of self-assembling into complex 3D macrostructures via DNA hybridization. Therefore, an effort was mounted to develop the materials and process required to enable generation of such materials. The goal of the work was photolithographically defined solid polymer parallelepipeds with facets that can be separately and directly functionalized with different sequences of ssDNA. These polyfunctionalized objects should be programmable such that different combinations of the specifically functionalized particles would self-assemble into complex 3D aggregate configurations, making it possible to build vast numbers of any conceivable macrostructure with minimum dimensions on the micrometer to nanometer scale.

The general process flow for fabricating these particles is outlined in Figure 1. First, a film stack consisting of a thick, patternable, and bioreactive copolymer over a thin sacrificial lift-off layer (LOL) is generated on a bare silicon wafer by spin-coating (Figure 1a). The first sequence of ssDNA (ssDNA A) is covalently bound to the surface of the copolymer (Figure 1b),

Received: November 3, 2013
Revised: January 10, 2014
Published: January 13, 2014

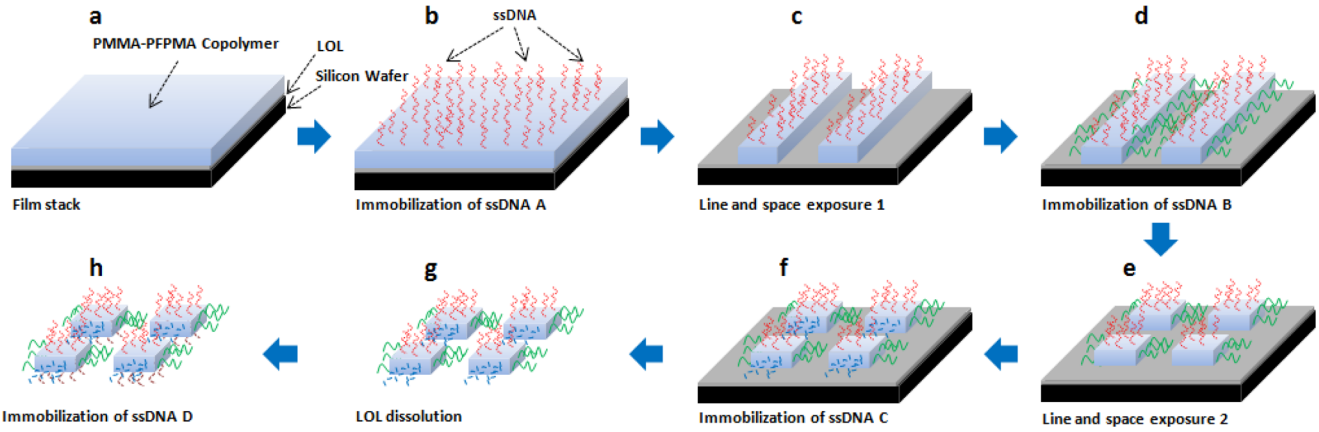

Figure 1. Fabrication process flow for ssDNA-functionalized polymer particles.

and then a blocking agent is applied to passivate any unreacted sites rendering them unreactive toward further covalent substitution. After the top surface of the film is functionalized and blocked, it is irradiated through a chromium-on-glass (COG) quartz photomask with large arrays of grating structures. The pattern is then developed to remove the irradiated regions. The sides of the line patterns present newly exposed reactive surfaces, which are then functionalized with a second ssDNA sequence (ssDNA B). Following a second blocking step, the mask is rotated 90°, and the film is irradiated again. Subsequent development yields large numbers of parallelepipeds whose newly exposed sides are then functionalized with ssDNA C followed by another blocking step. The particles are lifted off of the substrate by dissolving the LOL, and the suspended parallelepipeds are functionalized with ssDNA D. The process sequence depicted in Figure 1 produces particles with six different sides and four different (A–D) ssDNA functionalizations. Six different functionalizations can be achieved by employing a typical mask-to-substrate alignment system. The process for uniquely substituting all six sides is provided in the Supporting Information.

The major challenge associated with developing this process was in finding a combination of a copolymer, LOL, immobilization chemistry, developer, and stripper that are all compatible. This means that as soon as each working unit operation is established, it must be cross-checked for compatibility with the conditions of the other unit operations in order to be viable. For example, the LOL must not be appreciably soluble in the copolymer casting solvent, the ssDNA immobilization buffer, the blocking solution, or the developer. Likewise, the stripper for the LOL must not dissolve the copolymer or damage the ssDNA functionalized to the surface, and so forth. We report herein our progress in the development of the aforementioned process.

EXPERIMENTAL SECTION

Printing of Copolymer Polyfaceted Shapes. The first unit operation to be established was the dual-function copolymer because it is the key material for the success of the process and must have ability to act as both a photoresist and a bioreactive substrate. Methyl methacrylate was selected as the base monomer unit because PMMA homopolymer is a positive-tone photoresist at DUV wavelengths. Pentafluorophenyl methacrylate (PFPMA) was chosen as the bioreactive monomer unit because it has a contrast curve that is reasonably similar to that of the PMMA homopolymer (Figure 2). The pentafluorophenyl active ester can mediate direct amide bond formation with amine-terminated ssDNA. However, at the basic pH

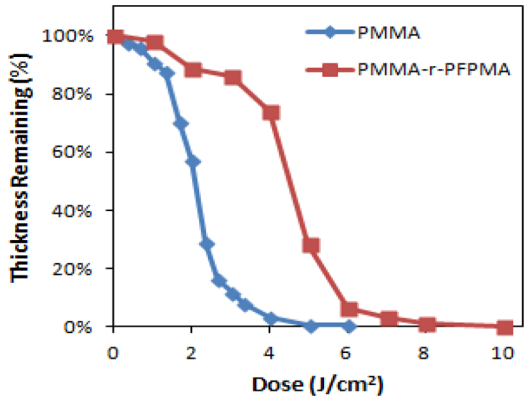

Figure 2. Contrast curve for PMMA and PMMA-r-PFPMA.

used in the coupling reaction, significant hydrolysis of the active ester occurred. Hence, the pentafluorophenyl group served only as a protecting group for the methacrylic acid and enabled solvent development under conditions that do not dissolve the LOL. The pentafluoro ester was hydrolyzed after patterning, and the amino terminal ssDNA was coupled using carbodiimide-based chemistry. This process gave far higher coupling yields than attempts to functionalize the surface directly by reaction of the active ester with amino-terminal ssDNA.

A copolymer composed of a 5:1 molar ratio of MMA to PFPMA was synthesized via free-radical polymerization using an AIBN initiator, dissolved in propylene glycol monomethyl ether acetate (PGMEA), and spin-coated at a thickness of 2.5 μm on a silicon wafer bearing a 200 nm thick lift-off layer of poly(methyl glutarimide) (PMGI). This film stack was then brought into full contact with a COG photomask and exposed to broad-band radiation from a 500 W mercury arc lamp (Oriel Instruments). After exposure, the film was immersed in a 1:3 v/v solution of methyl isobutyl ketone (MIBK) in isopropyl alcohol (IPA), which developed away all of the exposed copolymer to leave well-formed 5 × 5 × 2.5 μm^3 parallelepipeds of copolymer on the surface of the LOL. Optical micrographs of the structures produced by this process are provided in Figure 3.

These particles were removed from the surface of the wafer without significant attack on the copolymer surfaces using standard borate buffer-based photoresist stripper. The PMGI LOL (SF 5 grade, MicroChem) can be readily applied via spin-coating. This material is commonly used in semiconductor applications as a sacrificial undercut layer.[28] It wets and adheres to the silicon substrate and is compatible with the acrylate-based copolymer, making it an ideal candidate for the lift-off layer. The most critical characteristic of this material is that it is really soluble only in cyclopentanone and very basic stripper solutions, so it does not dissolve in the organic solvent mixture (MIBK/IPA)

dx.doi.org/10.1021/cm403637v | Chem. Mater. 2014, 26, 1457–1462

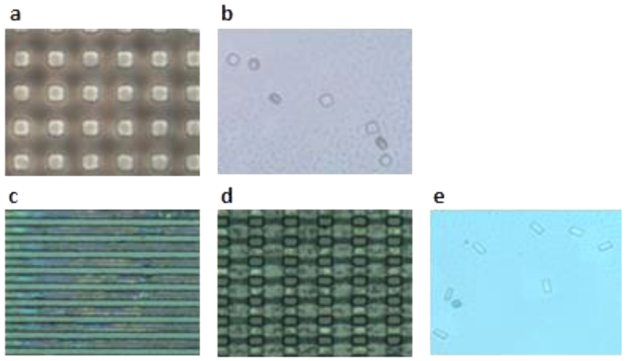

Figure 3. Optical microscope images of printed 5 × 5 μm^2 squares (a) in situ (on 200 nm PMGI LOL) and (b) in solution after lift-off. (c) Five micrometer line and space patterns in situ, (d) 5 × 10 μm^2 rectangles after 90° 10 μm line and space litho, and (e) 5 × 10 μm^2 rectangles in solution after lift-off.

that is used to develop the pattern printed in the reactive copolymer after exposure.

DUV exposure and development yielded the image in Figure 3a. Sections of the wafer (2 × 2 cm^2) were cleaved and placed face-up in 20 mL glass scintillation vials, and 100 μL of 1:4 potassium borate stripper solution (400k, Clariant) in water was dispensed onto the pattern in such a way as to maintain a sessile droplet confined to the area of the silicon chip. Release of the particles from the substrate was visible immediately to the naked eye, and after 2 min of carefully aspirating and redispensing the stripper for several cycles with a pipet, the stripper solution containing the particles was aspirated and transferred to a 1.5 mL centrifuge tube. The tube was centrifuged (Spectrafuge 7M, Labnet) for 60 s at 4000 rpm to yield a visible pellet. The stripper supernatant was removed, and the particles were rinsed four times by adding 100 μL of Millipore water, repeating the centrifugation and then removing the supernatant. An aliquot of the particles that was resuspended in Millipore water and dispensed onto a microscope slide is shown in Figure 3b. The process yielded large numbers of well-formed polymer particles.

Further performance testing of the PMGI LOL was required to show that it is capable of retaining the particles on the substrate not only through the development process but also through multiple ssDNA immobilization reactions, blocking reactions, and DUV exposures. For this purpose, a wafer was coated first with 200 nm of PMGI followed by with 2.5 μm of PMMA-PFPMA copolymer and then subjected to two perpendicular line-space exposures, two developer steps, four ssDNA immobilization reactions, and three blocking reactions, as outlined in Figure 1. The perpendicular exposures were 5 μm (Figure 3c) and 10 μm (Figure 3d) half-pitch gratings, respectively, yielding the rectangular shapes shown in Figure 3e after lift-off. The functionalization reactions were carried out in a pH 4.5 immobilization solution comprising 2-(*N*-morpholino)-ethanesulfonic acid (MES, Sigma-Aldrich) and 1-ethyl-3-(3-dimethylaminopropyl) carbodiimide (EDC, Sigma-Aldrich) for 12 h using the A_{FAM} sequence each time. To simulate the blocking reactions, the copolymer was subjected to the same 12 h immobilization solution but with an amine-terminal 5 bp sequence (NH_2−CGATG). The patterns were also immersed in 1% Tween-20 (Thermo Scientific) nonionic surfactant for 12 h to represent a worst-case scenario for the LOL.

After exposing the copolymer to all of these processing steps, a 60 s immersion in potassium borate readily released the particles into suspension. PMGI proved to be a very robust and versatile LOL for the purposes of generating ssDNA-functionalized particles. This material has the potential to be very useful in a wide variety of applications outside of the scope of this article.

Functionalization of the Particles with ssDNA. Carbodiimide-based amide bond formation is used extensively in Merrifield-like[29] processes for tethering amine-terminated oligomers and proteins to carboxyl-functionalized polymer beads. This chemistry was extended to PFPMA-containing polymers by first hydrolyzing the PFPMA group by immersing the particles in 50 mM phosphate buffer, pH 10, for 12 h to generate surface carboxylic acid functionalization. Fluorescently labeled amine terminal ssDNA was then coupled to this surface to analyze for the effectiveness of the ssDNA immobilization reaction. The details of the ssDNA sequences used in this report are shown in Table 1. The 5′ end of each strand was substituted with one of three different fluorophores for signal differentiation. The 3′ end of each strand was substituted with a primary amine group.

Sets of copolymer particles for the A_{FAM} and A'_{TYE} particles were printed, and the wafer chips were immersed in a functionalization solution comprising 45 μL of 100 mM MES, pH 4.5, along with 5 μL of 100 mM stock ssDNA solution (Integrated DNA Technologies) in Millipore water. A fresh batch of 1 M EDC in Millipore water was subsequently prepared, and 5 μL of that solution was added to the functionalization solution. After 12 h, the chips were consecutively immersed in solutions of 1× saline sodium phosphate EDTA (SSPE) buffer with 1% Tween-20 surfactant (Sigma-Aldrich), 1× SSPE, and Millipore water and dried. The particles were then lifted off of the chips with potassium borate and centrifuged into a pellet at 4000 rpm for 60 s, and then the supernatant was removed. Four rinse cycles were performed with Millipore water, resulting in a final suspension of the particles in 50 μL of water.

■ RESULTS AND DISCUSSION

Imaging flow cytometry was found to be a convenient analytical methodology for comparing the surface density of ssDNA on the particles. When the particles flow through the focused capillary of the cytometer (ImageStream, Amnis), they are excited by lasers at specific wavelengths and they emit light proportional to the amount of fluorophore-tagged ssDNA that there is on the surface. Histograms of the fluorescence intensity for each set of fluorophore-tagged particles are summarized in Figure 4 along with sample bright-field images and fluorescence images using two different filters. The camera channel 1 (Figure 4a,b) collects bright-field light that has been forward-scattered at low angles, which is translated into the pixel area of the particle. The camera channel 2 (Figure 4c,d) filter (400−470 nm) collects fluorescent light emitted from the FAM-labeled particles, and the channel 5 (Figure 4e and 4f) filter (595−660 nm) collects fluorescent light emitted from the Tye665-labeled

Table 1. List of ssDNA Sequences Used to Functionalize the Reactive Copolymer Surface Including the Fluorophore Emission Peak Wavelengths for Each Fluorophore[a]

name	5′ group	DNA sequence	3′ group	fluorophore emission (nm)
A_{FAM}	fluorescein (FAM)	$(AAAAA\ AAAAA)_5$	NH_2	540
A_{HEX}	hexachloro-fluorescein	$(AAAAA\ AAAAA)_5$	NH_2	555
A'_{TYE}	Tye665	$(TTTTT\ TTTTT)_5$	NH_2	665
B_{FAM}	fluorescein (FAM)	CCTCC CCTTT TATGC GTATG TATGC GTGCG TGCGT	NH_2	540
B'_{TYE}	Tye665	ACGCA CGCAC GCATA CATAC GCATA AAAGG GGAGG	NH_2	665

[a]A, adenine; T, thymine; G, guanine; and C, cytosine.

dx.doi.org/10.1021/cm403637v | *Chem. Mater.* 2014, 26, 1457−1462

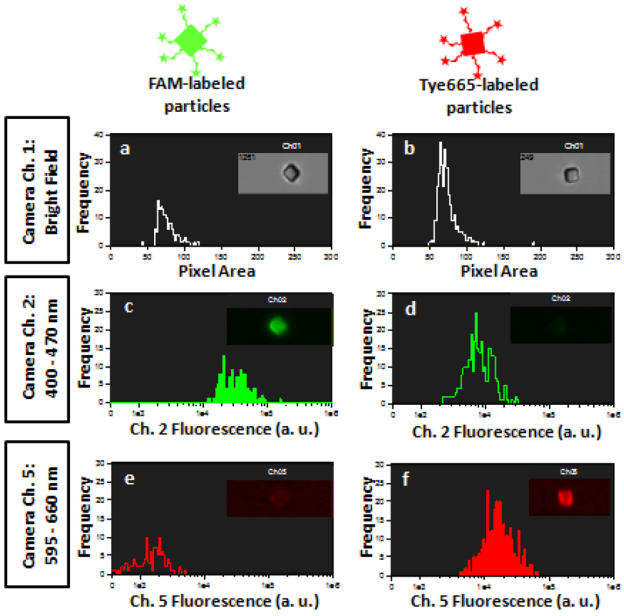

Figure 4. Flow cytometer fluorescence-intensity histograms and sample images for 2.5 × 5 × 5 μm^3 PMMA-co-PFPMA particles functionalized with either (a, c, e) A_{FAM} or (b, d, f) A'_{TYE} (columns). Histograms in panels a and b show area (bright field), c and d show fluorescent intensity at 400–470 nm (channel 2), and e and f show fluorescent intensity at 595–660 nm (channel 5) for both sets of particles.

particles. Each plot represents a log-scale frequency histogram of the scattered or fluorescent light signals for each particle or aggregate that passes in front of the laser beams.

The FAM-labeled A_{FAM} particles have a median fluorescence intensity of 3.2 × 10^4 a.u. for channel 2 and an intensity of 1.9 × 10^3 a.u. for channel 5. The Tye665-labeled A'_{TYE} particles have a median fluorescence intensity of 5.8 × 10^3 a.u. for channel 2 and an intensity of 1.7 × 10^4 a.u. for channel 5. The fact that the FAM-labeled particles produce a significant signal in the channel 5 camera filter and vice versa demonstrates that there is some cross-talk at each channel for each fluorophore but enough contrast exists to distinguish between the particle labeling. These data show that a significant density of fluorescent ssDNA has been bound to the surface of the particles. The PFPMA hydrolysis and subsequent carbodiimide immobilization are effective.

Particle Assembly. To confirm that the ssDNA surface functionalization is high enough to support particle–particle assembly under the shear forces present in agitated aqueous solutions and flow of the sort encountered in the cytometer, A_{FAM}-labeled parallelepipeds were functionalized in situ as previously described, lifted-off the substrate, and observed in both a mixture of A'_{TYE}-labeled 6 μm diameter carboxylate-modified polystyrene spheres (PolySciences, Inc.) and B_{FAM}-labeled polystyrene spheres via optical microscopy (BX60, Olympus) and imaging flow cytometry. The polystyrene spheres were functionalized in the same functionalization solution as the parallelepipeds, but the reaction was carried out in solution with 1200 rpm of agitation (Thermomixer, Eppendorf) for 2 h. Figure 5a is sample optical micrograph of a 1:4 mixture of A_{FAM} (parallelepipeds) and A'_{TYE} (spheres) cognate particles that were dispensed onto a microscope slide. Roughly 40% of the particles in the image are participating in assembly after just 30 s of agitation and approximately 1 min of

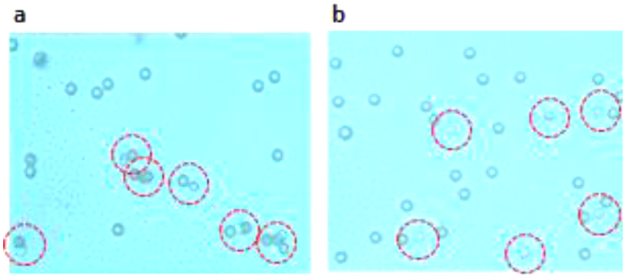

Figure 5. Optical micrographs of functionalized particle mixtures of (a) cognate A_{FAM} (parallelepipeds) and A'_{TYE} (spheres) and (b) noncognate A_{FAM} (parallelepipeds) and B_{FAM} (spheres). Parallelepipeds are marked with red dashed circles.

sedimentation, which is representative of approximately 30 images taken of the solution. A lack of particle–particle associations is clearly seen in Figure 5b for the A_{FAM} (parallelepipeds) and B_{FAM} (spheres) noncognate particle sets, indicating that the ssDNA on the surfaces of the particles is not readily participating in nonspecific hybridization events. Optical microscopy of the sedimented particles serves as a strong qualitative indicator of particle assembly for this platform.

Cognate (A'_{TYE} and A_{FAM}) and noncognate (A'_{TYE} and B_{FAM}) sets of parallelepiped copolymer particles were printed, functionalized in situ as previously described, and analyzed on an imaging flow cytometer to quantify the extent of the assembly as well as the specificity of the DNA hybridizations. The suspensions were combined and agitated for 30 s and then immediately loaded into the cytometer. The fluorescence intensity data for channels 2 and 5 for 1750 particles was plotted against each other as shown in Figure 6. The cross-talk

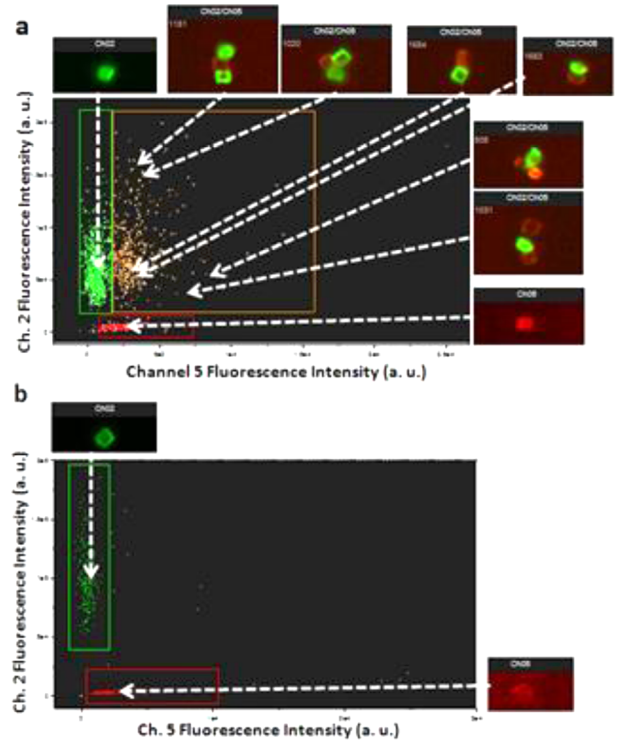

Figure 6. Fluorescence-intensity signals collected at channels 2 (FAM fluorescence) and 5 (Tye665 fluorescence) for (a) cognate and (b) noncognate particle mixtures on log–log scale.

dx.doi.org/10.1021/cm403637v | *Chem. Mater.* 2014, 26, 1457–1462

in the fluorescence data was compensated to yield horizontal and vertical data-point groups along the x and y axes, which represent the unassembled particles. The data points in between these groups, which produce strong fluorescent signals for both channels 2 and 5, represent assembly events. The cognate particle mixture in Figure 6a had a particle ratio of 1.5:1.0 (A'_{TYE}/A_{FAM}), a specific binding yield of 39.2%, and a binding selectivity ratio of 67.2:1.0 (positive/negative) compared to the noncognate control mixture (Figure 6b) that had a particle ratio of 1.5:1.0 (A'_{TYE}/B_{FAM}) and a specific binding yield of just 0.5%.

The cognate mixture participated in binding at a significant level, and, more importantly, the binding was very sequence-specific. The vast majority of the coupled particles were present in pairs; however, a very small amount of trimers and higher-order aggregates was also found. The noncognate mixture had very little assembly, and the few bound particles that did exist were mostly couplings from the same ssDNA group. Somewhat surprisingly, analysis of the individual assembly images indicates that the particles are not maximizing their local DNA hybridization areas. They appear to be coupling in seemingly random configurations instead of facet-to-facet configurations. This suggests that the particle associations are irreversible in nature, likely because of the high surface density of the immobilized ssDNA and the high melting temperatures of the complementary sequences used. These associations could be rendered more reversible by weakening the hybridization force of the DNA or decreasing the amount of surface-immobilized DNA present. The force of hybridization can be reduced by decreasing the length of the DNA strands, reducing their G−C base-pairing content, or raising the temperature of the solution during assembly. The amount of DNA present at the surface can be decreased by reducing the amount of PFPMA in the copolymer, thereby reducing the density of surface carboxyl groups available for DNA conjugation.

The configuration frequencies for the self-assembly of these particles are controlled by two factors. First, the focused flow in the thin 250 μm capillary in the cytometer imparts large shear forces on the flowing particles, causing larger and loosely coupled aggregates to disassemble before imaging. If the hybridization strength of the associations is too weak, then only solitary particles would be seen, which would render the tool useless. Conversely, if the association forces of the particles are too strong or if the shear forces imposed by the fluid flow in the capillary was too weak, then the very large particle aggregates would remain intact through the capillary or become so big that they would not fit through the capillary and therefore clog the instrument. However, the nature of the agitation of the particle sets during mixing influences the initial extent of hybridization of the particles. In general, lower particle concentrations, more aggressive mixing, and longer mixing times tend to lead to higher-order assembly products.

At this point, compatible, workable solutions for every unit operation in the process have been established with the exception of a process for passivating/blocking the residual carboxyl sites left available after each ssDNA immobilization. A blocking process is the key to localizing ssDNA on each facet of the shapes without allowing for cross-functionalization. Unfortunately, even after several repetitions of ssDNA functionalizations of the particles, the PMMA-PFPMA surface was never rendered completely unreactive. After repeated coupling reactions and apparent saturation of the fluorescence intensity, subsequent functionalization with a different sequence of ssDNA led to a significant amount of immobilization of the new sequence on the surface. A study in which carboxyl-functionalized polystyrene (PS) beads were functionalized multiple times in sequence with the A_{HEX} illustrates this problem. The pH 4.5 MES−EDC immobilization reaction of A_{HEX} was repeated nine times on 6 μm carboxyl-functionalized PS beads, and the fluorescence intensity leveled off with successive reactions. Then, the saturated beads were subjected to a single immobilization reaction with noncognate B'_{TYE}, and a surprising amount of Tye665 fluorescence was generated. Figure 7a is a plot of the median HEX fluorescence

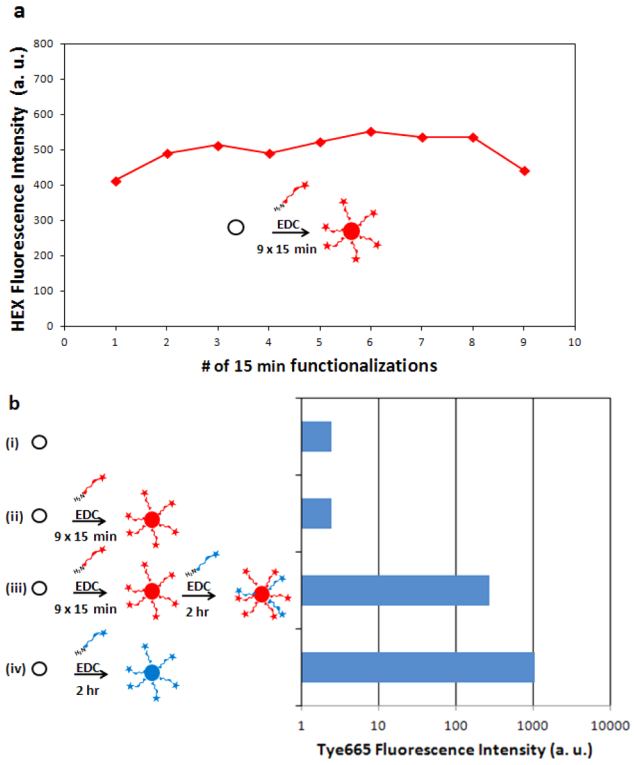

Figure 7. (a) Plot of the median HEX fluorescence intensity for 9× 15 min A_{HEX} functionalizations. (b) Log-scale bar chart of the median Tye665 fluorescence intensity for (i) naked 6 μm carboxyl PS beads, (ii) 9× A_{HEX}-labeled beads, (iii) 9× A_{HEX}-labeled beads followed by a single B'_{TYE} functionalization, and (iv) beads functionalized only with B'_{TYE} ssDNA.

of the PS beads run on a flow cytometer (FACSCalibur, BD Biosciences) after each reaction. The fact that the fluorescence intensity shows little increase with the successive reactions is what led to the assumption that all accessible reactive sites had been functionalized. Figure 7b is a bar chart of the median Tye665 fluorescence collected for a control sample of naked carboxyl PS beads (i), beads that underwent the 9× HEX ssDNA reaction (ii), beads that underwent the 9× HEX ssDNA reaction followed by a single Tye665 ssDNA reaction (iii), and a reference sample in which the naked beads were reacted with just the Tye665-labeled ssDNA (iv). It is apparent that the subsequent B'_{TYE} functionalization of the A_{HEX}-labeled beads results in a significant amount of Tye665 fluorescence, showing that these "exhaustively functionalized" beads are not fully immune to cross-functionalization.

Attempts to render these functionalized beads unreactive to subsequent ssDNA substitution, including reaction with a huge molar excess of such reagents as ethanolamine and even <5 bp

dx.doi.org/10.1021/cm403637v | Chem. Mater. 2014, 26, 1457−1462

ssDNA sequences, failed to block the unreacted sites. Efficient blocking is the key to achieving the desired end result and unfortunately, at the time of this writing, we have not found an effective means to achieve that result.

CONCLUSIONS

This article describes the successful development of a process for patterning polymer material that can produce free floating solid parallelepipeds in the sub 10 μm dimensional regime. It teaches how to immobilize ssDNA on the surface of the faces of these parallelepipeds at a density that enables sets of particles with cognate ssDNA to couple at a high rate upon agitation and to remain coupled even when subjected to the high shear stress present in a flow cytometer capillary. A robust LOL has been identified that is capable of withstanding several harsh processing steps without dissolving, including multiple organic developer steps, exposure steps, ssDNA functionalization steps, and blocking steps, and then can be selectively dissolved to free the functionalized particles. Use of dyes with different fluorescence spectra in conjunction with imaging flow cytometry enabled quantitative characterization of the self-assembly of the particles. Assembly results for a cognate mixture of the particles even under the high shear conditions in the flow cytometer demonstrated a coupling yield of approximately 39%. Results for a noncognate mixture showed that particles with mismatched ssDNA coupled at a very low rate (less than 1%), confirming the specific nature of the assembly. Unfortunately, despite extensive efforts, the establishment of a saturation/blocking procedure has not been fully successful. If such a process can be developed, then it would allow localization of specific ssDNA to the individual facets of polymer shapes, which would, in turn, surely enable efficient production of preprogrammed 3D structures for particle self-assembly.

ASSOCIATED CONTENT

Supporting Information

Aligned lithography process sequence for generating parallelepiped particles with six independently functionalized faces; lithography process details; image of broad-band DUV lithography platform showing the lamp, the shutter, and the protective box; image of the mask−substrate assembly positioned in front of the light source; EDC functionalization details; and reaction scheme for reacting amine-terminal single-stranded DNA with carboxyl groups on the surface of the copolymer particles (PDF). This material is available free of charge via the Internet at http://pubs.acs.org.

AUTHOR INFORMATION

Corresponding Author

*E-mail: willson@che.utexas.edu.

Author Contributions

The manuscript was written through contributions of all authors.

Notes

The authors declare no competing financial interest.

ACKNOWLEDGMENTS

This work was supported by the Rashid Engineering Regents Chair, the Welch Foundation (F-1654 and F-1830), the National Institutes of Health (EUREKA, 1-R01-GM094933), the National Security Science and Engineering Faculty Fellowship (FA9550-10-1-0169), the Virginia and Ernest Cockrell, Jr. Fellowship in Engineering, and the Larry Holmes − South Texas Section, Society of Plastics Engineers Endowed Presidential Fellowship in Chemical Engineering. We thank the UT Genome Sequencing and Analysis Facility and the UT ICMB Microscopy and Imaging Facility for equipment support.

REFERENCES

(1) Khodakov, D. A.; Thredgold, L. D.; Lenehan, C. E.; Andersson, G. A.; Kobus, H.; Ellis, A. V. *Proc. SPIE* **2011**, 82040J.
(2) Hsiao, S. C.; Shum, B. J.; Onoe, H.; Douglas, E. S.; Gartner, Z. J.; Mathies, R. A.; Bertozzi, C. R.; Francis, M. B. *Langmuir* **2009**, *25*, 6985.
(3) Li, J.; Fan, C.; Pei, H.; Shi, J.; Huang, Q. *Adv. Mater.* **2013**, *25*, 4386.
(4) Elghanian, R.; Storhoff, J. J.; Mucic, R. C.; Letsinger, R. L.; Mirkin, C. A. *Science* **1997**, *277*, 1078.
(5) Taton, T. A.; Mirkin, C. A.; Letsinger, R. L. *Science* **2000**, *289*, 1757.
(6) Sendroiu, I. E.; Warner, M. E.; Corn, R. M. *Langmuir* **2009**, *25*, 11282.
(7) Lämmerhardt, N.; Merzsch, S.; Ledig, J.; Bora, A.; Waag, A.; Tornow, M.; Mischnick, P. *Langmuir* **2013**, *29*, 8410.
(8) Braun, E.; Eichen, Y.; Sivan, U.; Ben-Yoseph, G. *Nature* **1998**, *391*, 775.
(9) Park, S. H.; Yan, H.; Reif, J. H.; LaBean, T. H.; Finkelstein, G. *Nanotechnology* **2004**, *15*, S525.
(10) Seeman, N. C. *J. Theor. Biol.* **1982**, *99*, 237.
(11) Chen, J. H.; Seeman, N. C. *Nature* **1991**, *350*, 631.
(12) Rothemund, P. W. K. *Nature* **2006**, *440*, 297.
(13) Deng, Z.; Tian, Y.; Lee, S.-H.; Ribbe, A. E.; Mao, C. *Angew. Chem.* **2005**, *117*, 3648.
(14) Tikhomirov, G.; Hoogland, S.; Lee, P. E.; Fischer, A.; Sargent, E. H.; Kelley, S. O. *Nat. Nanotechnol.* **2011**, *6*, 485.
(15) Le, J.; Pinto, Y.; Seeman, N.; Musier-Forsyth, K.; Taton, T. A.; Kiehl, R. *Nano Lett.* **2004**, *4*, 2343.
(16) Nykypanchuk, D.; Maye, M. M.; van der Lelie, D.; Gang, O. *Nature* **2008**, *451*, 549.
(17) Alivisatos, A. P.; Johnsson, K. P.; Peng, X.; Wilson, T. E.; Loweth, C. J.; Bruchez, M. P.; Schultz, P. G. *Nature* **1996**, *382*, 609.
(18) Ganachaud, F.; Elaissari, A.; Pichot, C. *J. Biomater. Sci., Polym. Ed.* **2000**, *11*, 931.
(19) DeKosky, B. J.; Ippolito, G. C.; Deschner, R. P.; Lavinder, J. J.; Wine, Y.; Rawlings, B. M.; Varadarajan, N.; Giesecke, C.; Dörner, T.; Andrews, S. F.; Wilson, P. C.; Hunicke-Smith, S. P.; Willson, C. G.; Ellington, A. D.; Georgiou, G. *Nat. Biotechnol.* **2013**, *31*, 166.
(20) Willner, I.; Cheglakov, Z.; Weizmann, Y.; Sharon, E. *Analyst* **2008**, *133*, 923.
(21) Oh, B.-K.; Nam, J.-M.; Lee, S. W.; Mirkin, C. A. *Small* **2006**, *2*, 103.
(22) Ramòn-Azcòn, J.; Yasukawa, T.; Mizutani, F. *Anal. Chem.* **2011**, *83*, 1053.
(23) Tang, H.; Deschner, R.; Allen, P.; Cho, Y.; Sermas, P.; Maurer, A.; Ellington, A. D.; Willson, C. G. *J. Am. Chem. Soc.* **2012**, *134*, 15245.
(24) Thurn, K. T.; Paunesku, T.; Wu, A.; Brown, E. M. B.; Lai, B.; Vogt, S.; Maser, J.; Aslam, M.; Dravid, V.; Bergan, R.; Woloschak, G. E. *Small* **2009**, *5*, 1318.
(25) Storhoff, J. J.; Lazarides, A. A.; Mucic, R. C.; Mirkin, C. A.; Letsinger, R. L.; Schatz, G. C. *J. Am. Chem. Soc.* **2000**, *122*, 4640.
(26) Walther, A.; Müller, A. H. E. *Chem. Rev.* **2013**, *113*, 5194.
(27) Qi, H.; Ghodousi, M.; Du, Y.; Grun, C.; Bae, H.; Yin, P.; Khademhosseini, A. *Nat. Commun.* **2013**, *4*, 2275.
(28) Young, S.; Weston, D.; Dauksher, B.; Mancini, D.; Pacheco, S.; Zurcher, P.; Miller, M. *J. Micromech. Microeng.* **2005**, *15*, 1824.
(29) Merrifield, R. B. *J. Am. Chem. Soc.* **1963**, *85*, 2149.